A Matching Technique Using Gradient Orientation Patterns

Toshiaki Kondo and Waree Kongprawechnon
Sirindhorn International Institute of Technology, Thammasat University
131 Moo 5, Tiwanont Road, Bangkadi
Pathum Thani 12000, Thailand
E-mail: tkondo@siit.tu.ac.th and waree@siit.tu.ac.th

Abstract

Time-varying lighting conditions cause temporal variations of image intensities and make most existing image matching techniques ineffective. As a solution to this irregular lighting condition problem, we propose a novel matching technique based on gradient orientation information in place of conventional image features such as intensities and gradients. Gradient orientation is known to be insensitive to variations of intensities. Gradient orientation information is utilized using two patterns that are obtained as the x and y components of unit gradient vectors. Simulation results show that the proposed matching technique is remarkably robust to both spatially uniform and non-uniform changes of image intensities.

Keywords: Image correspondence, block matching, template matching, cross correlation, and gradient orientation.

1. Introduction

Establishment of correspondence between two or more images is one of the most important tasks in image sequence processing and computer vision (also called machine vision and robot vision) applications. Establishing image correspondence is necessary to stitch multiple images to generate a new image with a wider view angle or to merge multiple images into one image with a higher spatial resolution. Furthermore, image correspondence is significant because it enables motion estimation and depth estimation. Motion estimation is concerned with the correspondence among time-sequential images, for instance, video sequences. Motion estimation is found in various applications, including object-based video coding (e.g. MPEG-4), object detection and tracking for surveillance systems, scene change detection for video editing, image stabilization for camcorders, etc. Meanwhile, depth estimation is more related to remote sensing that requires correspondence between images captured from different viewpoints at the same instant, such as, stereo vision. Depth estimation is a key technology for autonomous vehicles or robot navigation to understand 3-D environments. The acquisition of distance information in a 3-D scene for producing computer graphics is also a vital application of depth estimation.

Techniques for image correspondence in the spatial domain may be classified into two categories; gradient-based methods and matching methods. Gradient-based techniques can be further divided into two subgroups; the spatio-temporal gradient method (often simply referred to as gradient method or differential method) [1]-[3] and the gradient

structure tensor method (also referred to as gradient square tensor method or 3-D structure tensor method) [1], [4]-[9]. Gradient-based methods are in general used to obtain a dense optical flow field, or motion vectors. These techniques are effective, especially when the displacement between images over time is small, typically a few to several pixels. On the other hand, matching methods (also widely referred to as block matching, template matching, or correlation-based methods) may be a more intuitive and common approach, as they search for similar patterns between two images [1], [10]-[14]. Since matching methods can deal with large displacements between images, they are used not only for motion estimation, but also for depth estimation and the generation of a new image from multiple images.

One of our previous papers was related to gradient-based methods [19], while this paper is concerned with matching methods. Both approaches assume that the intensities of objects in an image are constant over time. This assumption, however, is often violated by changes in lighting conditions, that are a common occurrence in outdoor environments. To circumvent this irregular illumination problem, it is reasonable to employ a feature that is less dependent on image intensities. For this, gradient orientation or direction is an attractive feature because it is known to be insensitive to variations in illumination [15]-[18]. In this paper, we propose to use gradient orientation information for pattern matching, rather than relying on conventional image features such as intensities and gradients. A comparative study with conventional matching methods reveals that the proposed technique has a remarkable robustness to both uniformly and non-uniformly time-varying image intensities.

2. Gradient Orientation Information

As a robust image feature, we propose to use gradient orientation information (GOI) in place of conventional image features such as image intensities and gradients. We describe how to extract GOI from an image and make use of it in a computationally efficient manner.

2.1 Extraction of Gradient Orientation Information

Let $I(x, y)$ be the image intensities at pixel coordinates (x, y). The gradient vectors can then be expressed by (I_x, I_y) where I_x and I_y are the partial derivatives of $I(x, y)$ in the x and y directions. Fig. 1(a) shows $I(x, y)$, a standard test image, called Lena (or Lenna), of size 256 by 256 pixels with 256 gray levels. By convention, the upper left corner of the image is the origin, and vertical and horizontal axes are respectively denoted as x and y axes. The small region of size 32 by 32 pixels encompassed by a white square in Fig. 1(a) is cropped and enlarged in Fig. 1(b), while Fig. 1(c) shows the gradient vectors (I_x, I_y) within the cropped region.

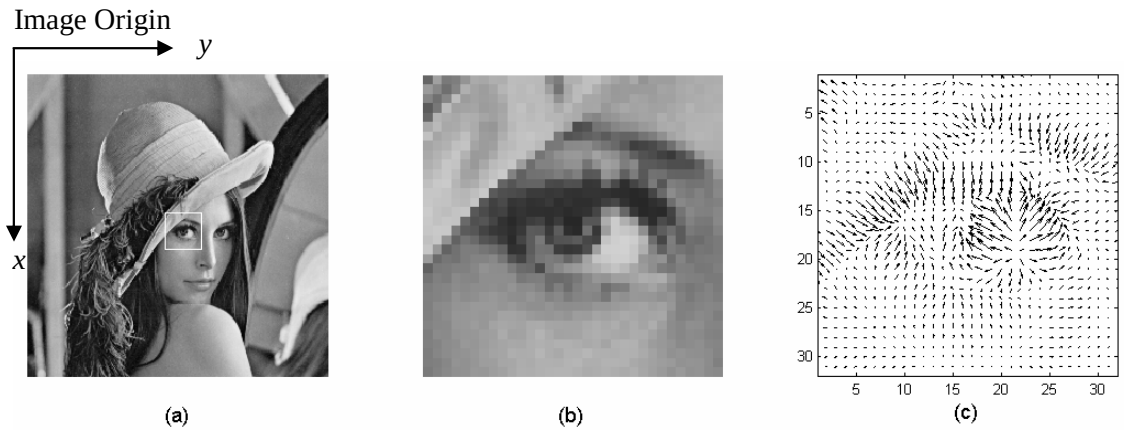

Fig. 1. (a) An 8-bit gray-scale image, $I(x,y)$, (b) a cropped and enlarged subimage, and (c) its gradient vectors, (I_x, I_y).

The gradient vectors (I_x, I_y) are represented by their magnitudes, i.e., norms, and orientations (or directions). GOI may be expressed using the unit gradient vectors (n_x, n_y) that can be obtained by dividing (I_x, I_y) by their norms:

$$\left.\begin{aligned} n_x(x,y) &= I_x(x,y) \Big/ \sqrt{I_x{}^2(x,y) + I_y{}^2(x,y)} \\ n_y(x,y) &= I_y(x,y) \Big/ \sqrt{I_x{}^2(x,y) + I_y{}^2(x,y)} \end{aligned}\right\}, \quad (1)$$

where we assign zeros to $n_x(x,y)$ and $n_y(x,y)$ if the denominator is close to zero to avoid zero division. As illustrated in Fig. 2, the unit gradient vectors (n_x, n_y) are represented by two scalars, n_x and n_y, with which we may process and utilize GOI. It should be noted that the use of unit gradient vectors is more computationally efficient than using angular values θ (rad) directly, because angular values require modulo calculations (e.g. difference between two angles cannot exceed π) [18].

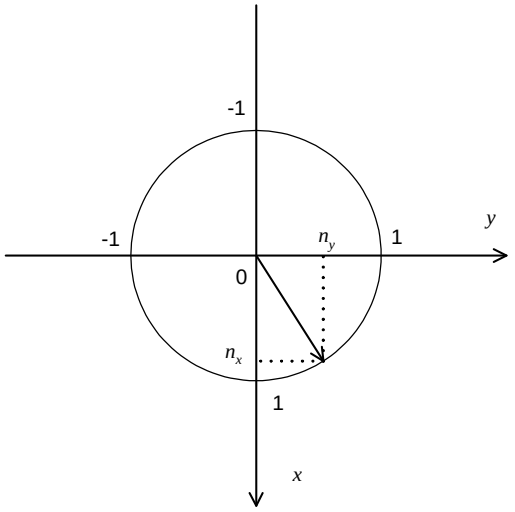

Fig. 2. A unit gradient vector (n_x, n_y).

Fig. 3(a) shows the unit gradient vectors of the cropped region in Fig. 1(b). Since n_x and n_y are scalars ranging from –1 to 1, they can be treated separately as input patterns as shown in Figs. 3(b) and 3(c), where n_x and n_y are scaled between 0 and 255 for visualization purposes. The unit gradient vectors in the bright regions in Fig. 3(b) are directed downward, i.e., the same direction as the x axis, while those in the dark regions point upward, i.e., the direction opposite to the x axis. Likewise, the unit gradient vectors in the bright areas in Fig.

3(c) point in the same direction as the y axis and those in the dark regions are directed leftward. In this way, GOI is now effectively represented with these two patterns, and we make use of these patterns for establishing image correspondence.

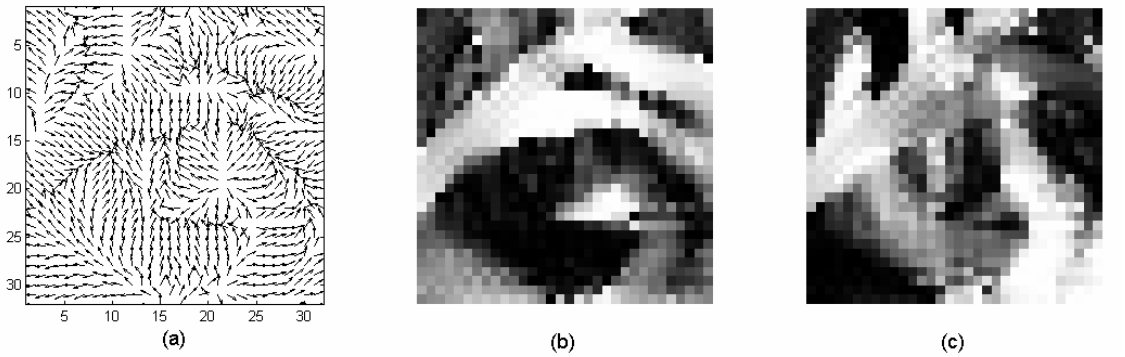

Fig. 3. (a) Unit gradient vectors (n_x, n_y), (b) a gradient orientation pattern of n_x, and (c) a gradient orientation pattern of n_y.

2.2 Intensity-invariance of Gradient Orientation

Fig. 4(a) shows the same subimage as in Fig. 1(b), except that the intensities of the upper half of it are reduced by 50%. Fig. 4(b) shows the gradient vectors of the subimage. The gradient vectors in the upper half are considerably different from those of Fig. 1(c) because of the changes of image intensities. This indicates the sensitivity of gradients to variations of image intensities. Fig. 4(c) shows the unit gradient vectors in the same region. Compared with the unit gradient vectors in Fig. 3(a), there are slight differences in the vicinity of the border of the shade added, but otherwise, they are identical to each other. Further, Figs. 4(d) and 4(e) show the gradient orientation patterns, n_x and n_y, of the subimage in Fig. 4(a). The differences between Fig. 3(b) and Fig. 4(d), and also the differences between Fig. 3(c) and Fig. 4(e) are seen only in a limited region around the boundary of the shade, and otherwise, these patterns are unchanged. Thus, it is evident that unit gradient vectors are insensitive to changes of image intensities and thus can maintain gradient orientation patterns well, regardless of varying illumination.

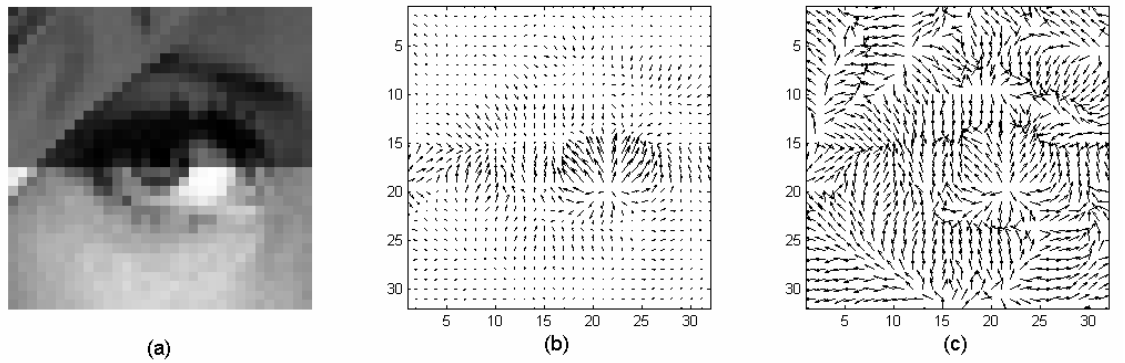

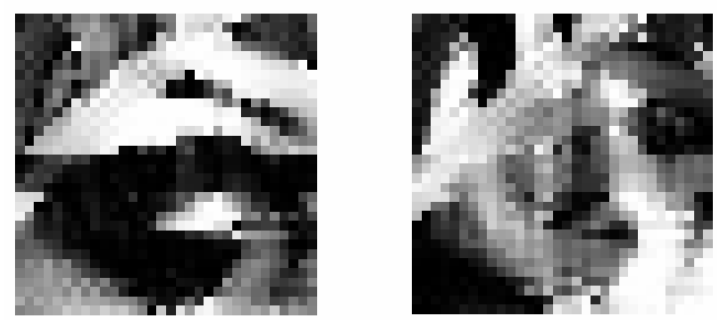

Fig. 4. (a) Subimage whose upper half is shaded, (b) gradient vectors, (c) unit gradient vectors, (d) a gradient orientation pattern n_x, and (e) a gradient orientation pattern n_y.

3. Matching Methods

In this section, we first review three conventional matching methods; 3.1 the block matching technique with the sum of absolute difference (SAD) criterion, 3.2 zero-mean normalized cross-correlation technique (ZNCC), and 3.3 a gradient vectors based matching technique with the gradient direction similarity measure (GD SM). The SAD matching technique provides both ease of implementation and good performance under regular lighting conditions. This technique is one of the most widely used methods for image matching. ZNCC is also a well-known matching technique and it has a great robustness to globally varying image intensities.

3.1 Block Matching Technique

In block matching methods, a reference image is partitioned into small blocks, and the corresponding region to each block, is then searched for in another image. The performance of the matching technique depends on the matching metric, the search strategy, the block size, and the features employed. This paper focuses on the last, the feature used for matching. The most commonly used matching method would be an image-intensity based block matching technique with the sum of absolute difference (SAD) metric (Eq. (2)):

$$SAD(\vec{p},\vec{d}) = \sum_{j=-N/2}^{N/2}\sum_{i=-N/2}^{N/2} \left| I_1(x+i,y+j) - I_2(x+i+u,y+j+v) \right| \quad (2)$$

where $\vec{p}$ denotes a point (x, y) in the image coordinate, $\vec{d}$ a displacement (u,v) from the point, equivalent to the displacement between the two images being used (or motion vectors if the two images are time sequential), N the block size, I_1 a block or template cropped at $\vec{p}$ from the first image (reference image), and I_2 the second image where a best-matching block is being searched for [1], [10], [12]. We use this SAD block matching technique for comparing with our proposed method because it is one of the most widely used matching techniques. From now on, we express this technique as SAD.

3.2 Zero-mean Normalized Cross-correlation Technique

Zero-mean normalized cross-correlation (ZNCC) is also a well-known metric for pattern matching:

$$ZNCC(\vec{p},\vec{d}) = \frac{\sum_{j=-N/2}^{N/2}\sum_{i=-N/2}^{N/2}\left\{I_1(x+i,y+j)-\overline{I_1}\right\}\left\{I_2(x+i+u,y+j+v)-\overline{I_2}\right\}}{\sqrt{\sum_{j=-N/2}^{N/2}\sum_{i=-N/2}^{N/2}\left\{I_1(x+i+u,y+j+v)-\overline{I_1}\right\}^2}\sqrt{\sum_{j=-N/2}^{N/2}\sum_{i=-N/2}^{N/2}\left\{I_2(x+i,y+j)-\overline{I_2}\right\}^2}}, \quad (3)$$

where the notations are the same as those in Eq. (2). *ZNCC* ranges from −1 to +1 depending on the similarity between two patterns under test [11], [12]. When two patterns are identical, the value of *ZNCC* becomes 1. Although ZNCC is based on image intensities, it is robust to both additive and multiplicative variations in intensities because the intensities are normalized as shown in Eq. (3). Hence, ZNCC is also selected as a method to compare, with the proposed method that has been designed to be robust to varying image intensities.

3.3 Gradient Vectors Based Matching Technique

Gradient vectors are also used as a robust feature for matching. The *x* and *y* components of the gradient vectors are used separately using the sum of absolute difference metric as:

$$\left.\begin{aligned} GDSM\_I_x(\vec{p},\vec{d}) &= \sum_{j=-N/2}^{N/2}\sum_{i=-N/2}^{N/2}\left|I_{x1}(x+i,y+j)-I_{x2}(x+i+u,y+j+v)\right| \\ GDSM\_I_y(\vec{p},\vec{d}) &= \sum_{j=-N/2}^{N/2}\sum_{i=-N/2}^{N/2}\left|I_{y1}(x+i,y+j)-I_{y2}(x+i+u,y+j+v)\right| \end{aligned}\right\}, \quad (4)$$

where I_{x1} and I_{y1} are the partial derivatives of the first image I_1 in *x* and *y* directions, and I_{x2} and I_{y2} the partial derivatives of the second image I_2, and other notations are the same as those in Eq. (2). Gradient direction similarity measure (GDSM) [14] is then given by:

$$GDSM(\vec{p},\vec{d}) = GDSM\_I_x(\vec{p},\vec{d}) + GDSM\_I_y(\vec{p},\vec{d}), \quad (5)$$

GDSM is similar to the proposed method in that both methods are based on gradient vectors in place of image intensities. Contrary to its name, however, GDSM depends not only on the directions (or orientations) of gradient vectors but also the magnitudes of them.

3.4 Gradient Orientation Pattern Matching Technique

The first two approaches, SAD and ZNCC, are based on image intensities, whereas gradient vectors are used in GDSM. These existing methods are all affected by varying lighting conditions because they are dependent on image intensities. In the proposed approach, we use unit gradient vectors, obtained through the normalization step as in Eq. (1), for establishing image correspondence. We call this technique the gradient orientation pattern based block matching (GOPM). Here, the widely used sum of absolute difference metric is employed as:

$$\left.\begin{aligned} GOPM\_n_x(\vec{p},\vec{d}) &= \sum_{j=-N/2}^{N/2}\sum_{i=-N/2}^{N/2}\left|n_{x1}(x+i,y+j)-n_{x2}(x+i+u,y+j+v)\right| \\ GOPM\_n_y(\vec{p},\vec{d}) &= \sum_{j=-N/2}^{N/2}\sum_{i=-N/2}^{N/2}\left|n_{y1}(x+i,y+j)-n_{y2}(x+i+u,y+j+v)\right| \end{aligned}\right\} \quad (6)$$

where n_{x1}, n_{y1} the unit gradient vectors in the first frame, i.e., the reference image I_1 and n_{x2}, n_{y2} those in the second frame I_2, and other notations are the same as those in Eq. (2). The difference between GDSM and GOPM lies in the fact that the former employs gradient vectors directly, while the latter uses unit gradient vectors. Thus, both

magnitudes and orientations of the gradient vectors are involved in GDSM, whereas only gradient orientation information is exploited in GOPM.

$$GOPM(\vec{p},\vec{d}) = GOPM\_n_x(\vec{p},\vec{d}) + GOPM\_n_y(\vec{p},\vec{d}) \quad . \quad (7)$$

We will compare the performances of SAD, ZNCC, GDSM, and the proposed technique, GOPM, in the next section.

4. Results and Discussion

We compare the motion estimation performance of SAD, ZNCC, GDSM, and GOPM on four standard test images; Lena (Fig. 1(a)), Girl (Fig. 5(a)), Cameraman (Fig. 5(b)), and House images (Fig. 5(c)). The test images have been converted to 8-bit gray-scale images of size 256 by 256 pixels for the comparative study. The test images serve as the first frames or reference images. The second image (next frame) for each test image is then generated by translating the test image by 5 pixels in both vertical and horizontal directions. Zero-mean Gaussian noise is then randomly generated and added to all image sequences where the SNR is approximately set to 40 dB. The intensities of the second image are modified in four ways, including realistic linear and Gaussian formed shadings [20], to evaluate the robustness of the four motion estimation techniques to varying illumination. We have computed 15 by 15, i.e., 225 motion vectors for each synthetic time-sequential image set. The block size is fixed at 16 by 16 pixels and the range for searching for the best matching position in the second image is limited to ±8 pixels both horizontally and vertically with the location of the block centre. We assume that motion estimation is successful only when an estimated motion vector is exactly 5 pixels, both vertically and horizontally. Tolerance to motion estimation error is not considered in this paper.

(a) (b) (c)

Fig. 5. Three more standard test images. (a) Girl, (b) Cameraman, and (c) House images.

Firstly, Table 1 shows the performances of the four matching techniques under a mildly noisy (40 dB) and uniformly varying lighting conditions where the image intensities of the second image are reduced to 80% (i.e., 20% darker). Figs. 6(a) and 6(b) show one of the four synthetic image sequences, and Figs. 6(c), 6(d), 6(e), and 6(f) show the motion vectors estimated by SAD, ZNCC, GDSM and GOPM, respectively. As shown in Table 1 and Fig. 6(c), it is apparent that SAD is very sensitive to a change of image intensities and completely failed to estimate motions correctly. The other three techniques can cope with a uniform change of image intensities very well (Table 1 and Figs. 6(d), (e), (f)). Fig. 6(f) shows, however, that the performance of GOPM is rather poor at extremely low-contrast areas (sky), compared with ZNCC

and GDSM. GOPM utilizes gradient orientation information in the form of unit gradient vectors that are obtained by dividing the magnitudes of gradient vectors (Eq. (1)). Because of this division, GOPM tends to be more susceptible to noise where image contrast is very low, i.e., flat areas corresponding to, for example, sky and walls. This may be a possible weakness of GOPM.

Table 1. Successful motion estimation rates (%) of 225 motion vectors estimated by SAD, ZNCC, GDSM, and GOPM for the true motion of (5, 5) pixels under mildly noisy (40 dB) and changing lighting condition where the second image is 20% darker than the first image uniformly.

Images	SAD	ZNCC	GDSM	GOPM
Lena	25.3	100	100	100
Girl	28.4	100	100	100
Cameraman	37.3	99.6	100	97.3
House	4.89	98.2	97.8	90.7

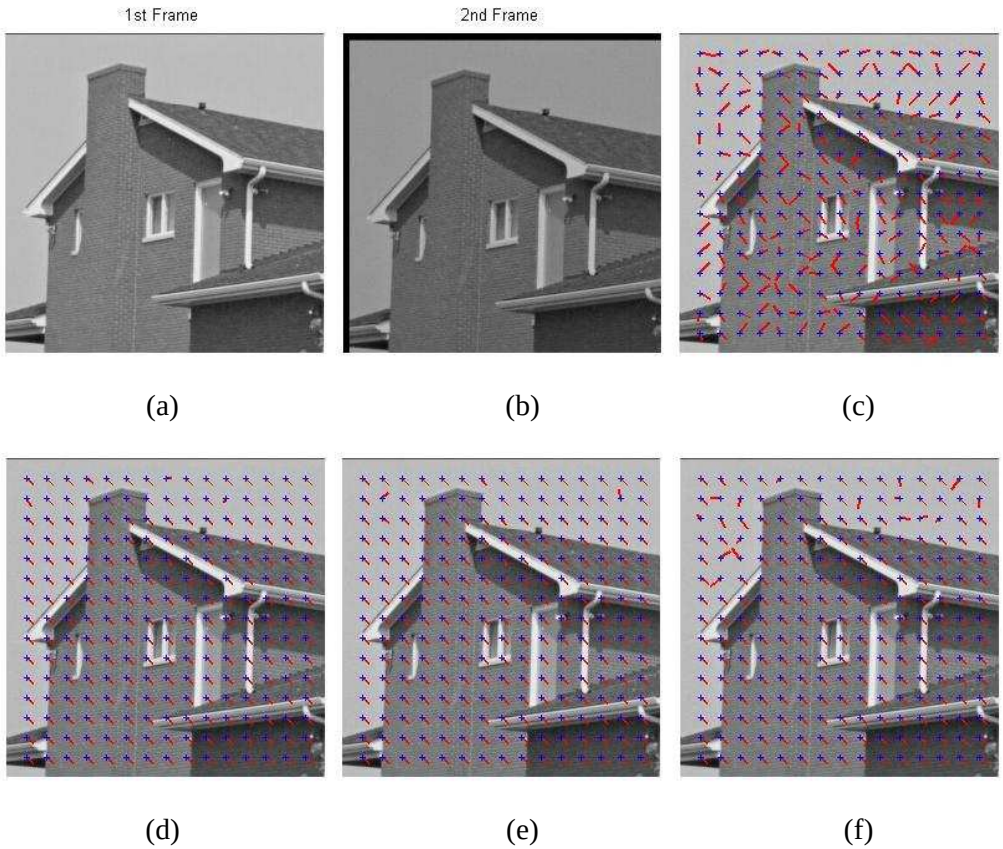

Fig. 6. (a) The first image (an original test image) used as a reference, (b) the second image generated by translating the original image by (5, 5) pixels and reducing intensities by 20%, and motion vectors estimated by (c) SAD, (d) ZNCC, (e) GDSM, and (f) GOPM.

Secondly, the intensities of the second image are reduced linearly in the right direction. The intensities are reduced up to 50% at the rightmost column of the image (Fig. 7(b)). Other conditions, including SNR, are the same as those of the simu-

lation above. As shown in Table 2 and Fig. 7, the second simulation results are almost identical to those in Table 1 and Fig. 6, in that SAD hardly works properly (Fig. 7(c)), while ZNCC (Fig. 7(d)), GDSM (Fig. 7(e)), and GOPM (Fig. 7(f)) perform very well despite the linear shading added. Erroneous motion estimation results by GOPM are seen in the sky in Fig. 7(f), showing the sensitivity of the method to low contrast.

Table 2. Successful motion estimation rates (%) of 225 motion vectors estimated by SAD, ZNCC, GDSM, and GOPM for the true motion of (5, 5) pixels under mildly noisy (40 dB) and non-uniform changes of image intensities where the image intensities are linearly reduced to half toward the right end of the image.

Images	SAD	ZNCC	GDSM	GOPM
Lena	26.2	99.1	99.6	100
Girl	25.8	100	100	100
Cameraman	40.0	99.6	99.6	97.8
House	4.88	96.9	96.0	90.7

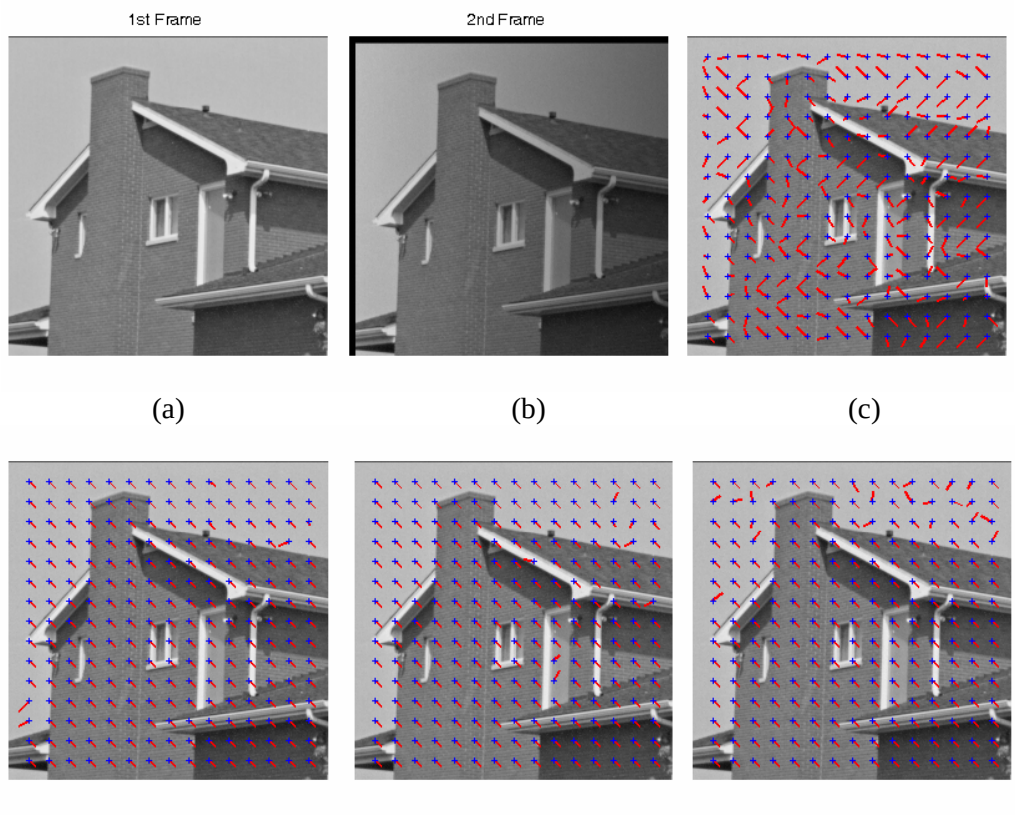

Fig. 7. (a) The first image (an original test image) used as a reference, (b) the second image generated by translating the original image by (5, 5) pixels and linearly reducing the intensities up to 50% in the right direction, and motion vectors estimated by (c) SAD, (d) ZNCC, (e) GDSM, and (f) GOPM.

Thirdly, the intensities of the second image are modified in such a manner that a Gaussian function is multiplied to the image and a gray scale offset of 50 is added. The

peak of the Gaussian function coincides with the center of the image, and thus the intensities are reduced toward the outskirts of the image (Fig. 8(b)). Other conditions, such as SNR (40dB), are the same as before. As shown in Table 3 and Fig. 8(c), SAD works correctly only in the center part of the image because the changes of intensities in there are limited. The success rates of SAD, however, are far from satisfactory. The other three techniques work well in general. Most erroneous motion estimation occurs in a low contrast area (sky), which highlights the difficulty in the accurate motion estimation in the absence of image gradients.

Table 3. Successful motion estimation rates (%) of 225 motion vectors estimated by SAD, ZNCC, GDSM, and GOPM for the true motion of (5, 5) pixels under mildly noisy (40 dB) and non-uniform changes of image intensities where the image intensities are multiplied with a Gaussian function and adding a gray scale offset.

Images	SAD	ZNCC	GDSM	GOPM
Lena	44.9	97.8	99.1	99.6
Girl	21.8	100	99.6	99.6
Cameraman	36.4	99.1	98.2	95.1
House	40.0	92.0	86.7	83.1

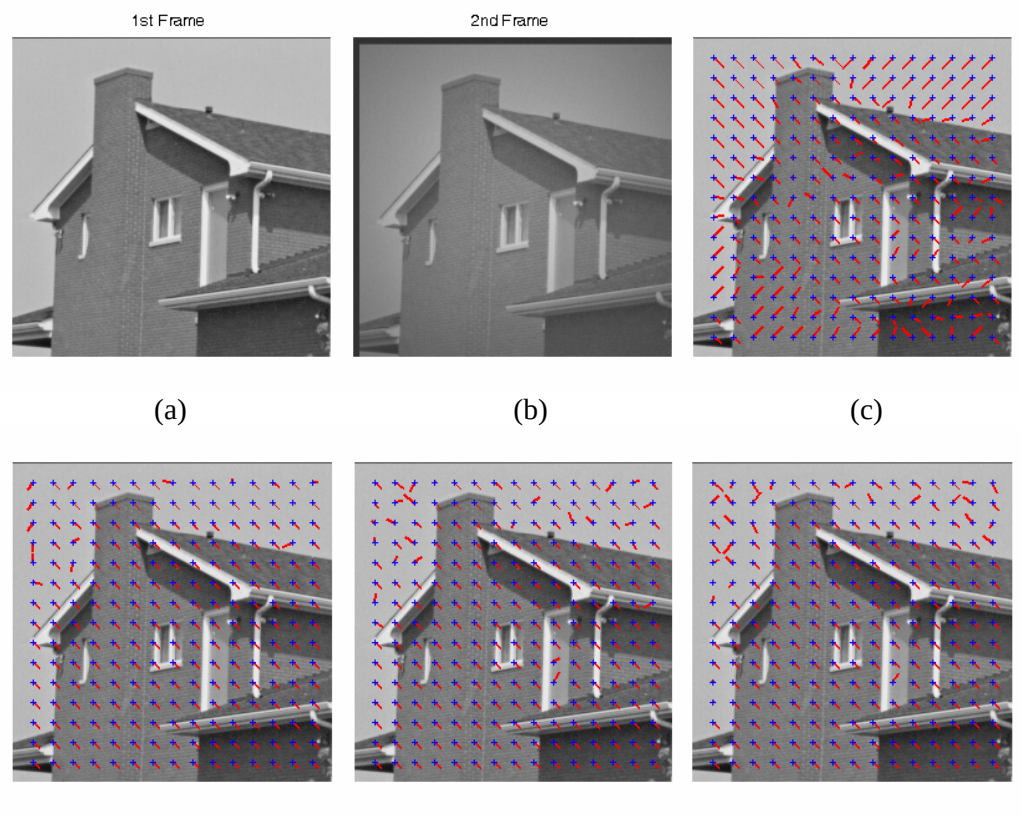

Fig. 8. (a) The first image (an original test image) used as a reference, (b) the second image generated by translating the original image by (5, 5) pixels, multiplying a Gaussian function, and adding a gray scale offset, 50, and motion vectors estimated by (c) SAD, (d) ZNCC, (e) GDSM, and (f) GOPM.

In the fourth simulation, the intensities in the second image are rapidly reduced to half within vertical and horizontal stripes while the intensities in the intersections of these stripes are reduced to 25%, i.e., 75% darker (Fig. 9(b)). Other conditions, such as SNR (40dB), are the same as before. As shown in Table 4 and Fig. 9(c), SAD fails to work correctly under varying lighting conditions and all the blocks in the first image are drawn to areas with similar intensities rather than to similar patterns in the second image. ZNCC overcomes varying illumination problems when a change of lighting conditions occurs uniformly within a block where ZNCC is computed, but when a change of image intensities occurs non-uniformly within the block, as shown in Fig. 9(b), it is not as effective as expected any longer (Fig. 9(d)). GDSM shows a considerable improvement over ZNCC, especially where there are sufficient gradients in the image, but many false motion vectors are seen in plain areas (Fig. 9(e)). Since GDSM uses gradient vectors, i.e., both gradient magnitude and orientation, it is still dependent on image intensities and is thus susceptible to varying illumination. Therefore, the false motion vectors seen in the sky are similar to those of SAD. Finally, Fig. 9(f) shows the motion vectors obtained by GOPM. Correct motion vectors are detected in almost all the blocks, except for extremely low-contrast areas. The comparison among the four methods clearly shows the remarkable robustness of GOPM to even rapid variations of image intensities.

Table 4. Successful motion estimation rates (%) of 225 motion vectors estimated by SAD, ZNCC, GDSM, and GOPM for the true motion of (5, 5) pixels under mildly noisy (40 dB) and non-uniform changes of image intensities where the image intensities within vertical and horizontal stripes are rapidly reduced to half and the intensities in the areas where two stripes overlap are reduced to one fourth.

Images	SAD	ZNCC	GDSM	GOPM
Lena	10.2	20.0	68.9	95.1
Girl	13.3	26.7	88.4	94.2
Cameraman	13.8	29.3	59.6	82.2
House	1.78	5.78	49.8	76.9

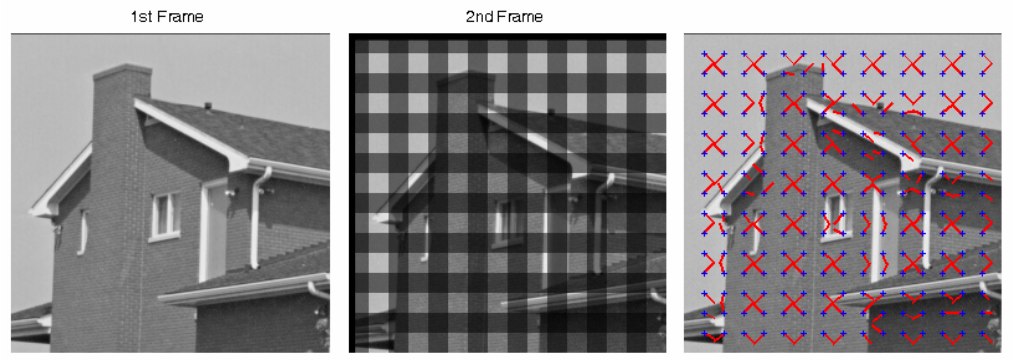

(a) (b) (c)

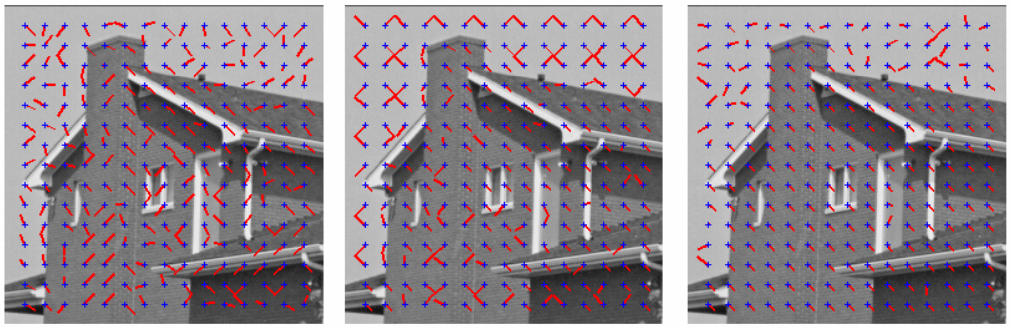

(d) (e) (f)

Fig. 9. (a) The first image (an original test image) used as a reference, (b) the second image generated by translating the original image by (5, 5) pixels and reducing intensities by 50% (within stripes) and 75% (intersections of the stripes), and motion vectors estimated by (c) SAD, (d) ZNCC, (e) GDSM, and (f) GOPM.

Finally, we compare the performances of the four matching techniques on a real video sequence. Figs. 10(a) and 10(b) show two time-sequential images that are cropped from a video sequence with the resolution of 256 by 256 pixels and of 8-bit gray levels. The first image is shot without flashlight and the second with flashlight. Consequently, the brightness of the faces in the images changes non-uniformly to a great extent. Besides the change in intensities, the second image is almost uniformly shifted in the low right direction from the first image. Fig. 10(c) shows the motion vectors estimated by SAD. All the motion vectors in the areas subjected to intensity changes due to the flashlight are erroneous. Fig. 10(d) shows the motion vectors estimated by ZNCC in which several erroneous motion vectors are seen on the face of the girl in the image. Fig. 10(e) shows the motion vectors estimated by GDSM. The results are similar to those of ZNCC, but more erroneous vectors are seen on the girl's face and her jacket. Lastly, Fig. 10(f) shows the motion vectors estimated by GOPM. Although a few erroneous motion vectors are found, the estimated motion vectors are largely uniform and match well the perceptible image motion of the video sequence. Since there are no reference data about image motion available for real images, as an attempt for numerical comparison,we evaluate the smoothness of the motion vectors estimated by the four approaches. Because the images are shifted almost uniformly, probably due to the cameraman's hand shaking, the standard deviation (SD) of correct motion vectors should be small. If there are many false motion vectors, the SD of those estimated vectors will be large. Table 3 lists the SDs of the x and y components of the 225 motion vectors estimated by the four methods, and their averages. SAD shows the largest SDs which proves the low reliability of the method under varying lighting conditions. Although the SDs of ZNCC and GDSM are much smaller than those of SAD, GOPM shows the smallest SD, which indicates the least faulty motion estimations among the four matching techniques. The comparison among the four matching techniques on the real image sequence accords well with the simulation results on the four synthetic image sequences. Thus, the robustness of GOPM to varying image intensities has been verified on both a synthetic image sequences and a real video sequence.

Fig. 10. (a) The first image used as a reference, (b) the second image with flashlight, and motion vectors estimated by (c) SAD, (d) ZNCC, (e) GDSM, and (f) GOPM.

Table 5. The standard deviations of the motion vectors estimated by SAD, ZNCC, GDSM, and GOPM in pixel units.

Standard deviations (SD)	SAD	ZNCC	GDSM	GOPM
SDs of *x* components of estimated motion vectors	3.03	2.26	2.48	1.45
SDs of *y* components of estimated motion vectors	3.29	1.76	1.76	1.80
Averages of the two SDs above	3.16	2.01	2.12	1.63

In addition to the evaluation on the performances of the four motion estimation techniques, we have compared the computational costs of them. Table 6 shows the computation time of each method for computing 225 motion vectors in a test image of size 256 by 256 pixels. The four techniques are implemented in MATLAB (Version 7.0) and executed on a PC with the Pentium 4 (2.80GHz) and 1GB of RAM. SAD is the fastest method among the four because the definition of the similarity measure in Eq. (2) is the simplest. It should be noted that both GDSM and GOPM are nearly as fast as SAD, though these require two subtractions as in Eqs. (4) and (6) in contrast to only one subtraction for SAD. Since these subtractions can be performed using 8-bit integers after an appropriate scaling process, their computational costs

are not significant. GOPM requires an extra computation of Eq. (1). However, since this step needs to be performed only once after loading an image, the impact on the additional computation is negligible. ZNCC, on the other hand, is the slowest because of its complex computation of Eq. (3), that requires repeated computations of multiplications and divisions.

Table 6: Computation times of the four motion estimation methods; SAD, ZNCC, GDSM, and GOPM.

	SAD	ZNCC	GDSM	GOPM
Computation time (sec)	2.44	4.41	2.56	2.56

5. Conclusions

Most existing approaches for image matching are based on either image intensities or gradient vectors. Consequently, it is inevitable that these conventional matching techniques are susceptible to varying image intensities caused by irregular illumination conditions. To cope with this illumination problem, we have presented a novel matching technique that is based on gradient orientation patterns that can be obtained as the x and y components of unit gradient vectors. We do not use the angular values θ (rad) of gradient vectors directly to evade modulo computation, which makes a fast implementation of the proposed method possible. Simulation results on both synthetic and real image sequences have revealed that the proposed technique, GOPM, is remarkably robust to varying image intensities compared with the conventional motion estimation techniques, SAD, ZNCC, and GDSM. A significant advantage of GOPM is that it can cope with not only global and often slow variations of image intensities, but also local and often rapid variations of image intensities that may be a common occurrence in outdoor environments. Gradient vectors are generally computed at an early stage of various image processing and computer vision applications, and are readily available. The normalization of the gradient vectors to obtain the unit gradient vectors can be performed prior to the computation for image correspondence. Therefore, the proposed techniques will be well-suited to real-time applications and also hardware implementation. We plan to evaluate the performance of GOPM further using more real image sequences containing local motions.

6. Acknowledgements

This research work is supported by research grants from the Thammasat University Research Fund and the Thailand Research Fund (MRG5180364). The authors are also grateful to the anonymous reviewer for his/her constructive comments and suggestions for improving this paper.

7. References

[1] Reed TR, *Digital Image Sequence Processing, Compression, and Analysis*. CRC Press, 2005.

[2] Horn BKP and Schunck BG, Determining Optical Flow. *Artificial Intelligence*, pp. 185-203, 1981.

[3] Kearney JK, Thompson WB, and Boley DL, Optical Flow Estimation: An Error Analysis of Gradient-based Methods with Local Optimization. *IEEE Trans. Pattern Anal. Machine Intell.*, Vol. 9, No. 2, pp. 229-244, 1987.

[4] Westin CF and Knutsson H, Estimation of Motion Vector Fields Using Tensor Field Filtering. *Proceedings of the IEEE Int'l Conf. on Image Processing*, 2, pp. 237-241, 1994.

[5] Zhang J, Gao J, and Liu W, Image Sequence Segmentation Using 3-D Structure Tensor and Curve Evolution. *IEEE Trans. Circuits and Syst. for Video Tech.*, Vol. 11, No. 5, pp. 629-641, 2001.

[6] Spies H and Scharr H, Accurate Optical Flow in Noisy Image Sequences. *Proceedings of the IEEE Int'l Conf. on Computer Vision*, pp. 587-592, 2001.

[7] Liu H, Chellappa R, and Rosenfeld A, Accurate Dense Optical Flow Estimation Using Adaptive Structure Tensors and A Parametric Model. *IEEE Trans. Image Processing*, Vol. 12, No. 10, pp. 1170-1180, 2003.

[8] Strzodka R and Garbe C, Real-Time Motion Estimation and Visualization on Graphics Cards, *IEEE Visualization*, pp. 545-552, 2004.

[9] Pless R and Wright J, Analysis of Persistent Motion Patterns Using the 3D Structure Tensor. *Proceedings of the IEEE Workshop on Motion and Video Computing*, 2, 2005.

[10] Jain R, Kasturi R, and Schunck BG, *Machine Vision*, McGraw-Hill, Inc., 1995.

[11] Gonzalez RC and Woods RE, *Digital Image Processing*, Prentice-Hall, Inc., 2002.

[12] Giachetti A, Matching Techniques to Compute Image Motion. *Image and Vision Computing*, 18, pp. 247-260, 2000.

[13] Ye M, Haralick RM, and Shapiro LG, Estimating Piecewise-Smooth Optical Flow with Global Matching and Graduated Optimization. *IEEE Trans. Pattern Anal. Machine Intell.*, Vol. 25, No. 12, pp. 1625-1630, 2003.

[14] Alkaabi S and Deravi F, Gradient Direction Similarity Measure. *Electronics Letters*, Vol. 39, No. 23, 2003.

[15] Gregson PH, Using Angular Dispersion of Gradient Direction for Detecting Edge Ribbons, *IEEE Trans. Pattern Anal. Machine Intell.*, Vol. 15, No. 7, pp. 682-696, 1993.

[16] Kondo T and Yan H, Automatic Human Face Detection and Recognition under Non-Uniform Illumination, *Pattern Recognition*, 32, pp. 1707-1718, 1999.

[17] Chen HF, Belhumeur PN, and Jacobs DE, In Search of Illumination Invariants, *Proceedings of the IEEE Int'l Conf. on Comp. Vision and Pattern Recognition*, 1, pp. 254-261, 2000.

[18] Burgi PY, Motion Estimation Based on the Direction of Intensity Gradient. *Image and Vision Computing*, 22, pp. 637-653, 2004.

[19] Kondo T, Boonsieng P, and Kongprawechnon W, Improved Gradient-Based Methods for Motion Estimation in Image Sequences, *SICE International Annual Conference on Instrumentation, Control and Information Technology*, Tokyo, August 2008.

[20] Kim YH, Martinez AM, and Kak AC, Robust Motion Estimation under Varying Illumination, *Image and Vision Computing*, 23, pp. 365-375, 2005.